5408–5415 Nucleic Acids Research, 1994, Vol. 22, No. 24

Non-covalent DNA groove-binding by 2-amino-1-methyl-6-phenylimidazo[4,5-*b*]pyridine

Glenn A.Marsch, Raymond L.Ward[1], Michael Colvin[2] and Kenneth W.Turteltaub*
Biology and Biotechnology Research Program, L-452 and [1]Department of Chemistry and Materials Science, L-310, Lawrence Livermore National Laboratory, Livermore, CA 94551 and [2]Department of Computational Engineering, Sandia National Laboratories, Livermore, CA 94551, USA

Received July 21, 1994; Revised and Accepted October 4, 1994

ABSTRACT

The cooked meat mutagen 2-amino-1-methyl-6-phenylimidazo[4,5-*b*]pyridine (PhIP) is metabolized *in vivo* to electrophilic intermediates that covalently bind to DNA guanines. Here we address the mechanism of PhIP's non-covalent interaction with DNA by using spectroscopic and computational methodologies. NMR methodologies indicated that upon addition of DNA, PhIP aromatic protons underwent a small, 0.11 – 0.12 p.p.m. upfield shift. DNA phosphorus resonances of non-covalent PhIP – DNA complexes broadened and slightly shifted upfield, while DNA base imino proton resonances shifted slightly downfield relative to DNA alone. UV and fluorescence spectra of PhIP titrated with DNA showed no detectable shifting and hypochromism of absorbance or fluorescence bands. In the presence of DNA, PhIP fluorescence was efficiently quenched by acrylamide, but not by silver ion. Further, the NMR spectra suggest that PhIP is in fast exchange with the DNA, and is slightly specific for adenine – thymine (A – T) sequences. Finally, structural arguments based on quantum chemistry calculations suggested that PhIP and its metabolites are unlikely to intercalate into DNA. These data collectively indicate that PhIP non-covalently binds in a groove of DNA.

INTRODUCTION

The amino-imidazoazaarenes (AIAs) are a class of heterocyclic amine compounds formed during pyrolysis of protein by condensation of creati(ni)ne with amino acids (1,2). AIAs have been found in cooked muscle meats (3–5), but have been detected at lower levels in food products, e.g. processed grains, beer and wine (6,7). In addition, AIAs have been identified in tobacco smoke condensate (8) and in the urine of smokers (9). Importantly, some of these compounds are highly mutagenic (4,10,11,12): potencies of 23 to $\sim 10^6$ TA538 revertants/μg AIA have been reported by the Ames/*Salmonella* assay, with 2-amino-3,4-dimethylimidazo[4,5-*f*]quinoxaline (4-MeIQx) having the highest known mutagenic potential (4,11,12). Thus, AIA exposure is a component of the Western lifestyle and may pose a considerable human health risk.

2-amino-1-methyl-6-phenylimidazo[4,5-*b*]pyridine (PhIP) is basically the predominant AIA formed in cooked meat (3,13). PhIP is over two orders of magnitude less mutagenic than 4-MeIQx in *Salmonella typhimurium* (4,14), but is highly mutagenic in mammalian cells (15,16), and induces breast and colon cancers in rats (17–19), and lymphomas in mice (19,20). Germane to studies of human cancer risk is that the gastrointestinal tract of humans may be a target for PhIP-induced carcinogenesis.

PhIP is not carcinogenic *per se*, but is activated *in vivo* predominantly by cytochrome P4501A enzymes (21). The resulting *N*-hydroxy intermediate (21–24) then becomes a substrate for cellular sulfotransferases, acetyltransferases, and other conjugating enzymes (24–26). The enzyme-catalyzed conjugation of *N*-OH-PhIP by the transferases yields a PhIP intermediate esterified through the *N*-OH functionality to a reactive group, e.g., *N*-O-acetyl-PhIP (24–26). These metabolites are unstable electrophiles that are reactive towards DNA, resulting in facile formation of DNA adducts at guanines *in vivo* (25,27,28) and *in vitro* (24).

The PhIP–DNA adducts are presently being intensely studied. Postlabeling analyses suggest that two to three major PhIP adducts are likely formed in most tissues (24). Only one, the N^2-(2′-deoxyguanosin-8-yl)-PhIP adduct, has been unambiguously identified by ^{1}H NMR and mass spectrometry (29,30). However the related heterocyclic amine mutagens 2-amino-3,8-dimethylimidazo[4,5-*f*]quinoxaline (8-MeIQx) and 2-amino-3-methylimidazo[4,5-*f*]quinoline (IQ) have been reported to covalently bind at the N^2-NH_2 of guanines as well as at the C-8 position (31).

The formation of covalent DNA lesions typically follows the physical (non-covalent) association of the carcinogen and the DNA, although it is not clear to what degree non-covalent binding directs adduction (32). For polycyclic aromatic carcinogens that form bulky aromatic DNA adducts, e.g. aflatoxin B_1 (33) or (+)-*anti*-benzo[*a*]pyrene diol epoxide (BPDE) (32,34), these

*To whom correspondence should be addressed

complexes may form by intercalation before covalent substitution into DNA bases occurs. No data has previously been reported which verifies the mode of DNA binding by PhIP. In this paper, we report on the non-covalent interaction of unsubstituted PhIP with DNA. PhIP, and not its metabolites, was utilized in these studies because of the lability of either *N*-sulfonyl or *N*-acetoxy-PhIP. The resulting data, based on UV, fluorescence, ^{31}P NMR, and ^{1}H NMR (lowfield region) spectroscopies, indicate that PhIP groove-binds to DNA under the conditions used in this study. Of course the mode of DNA binding by PhIP could be different from that of PhIP metabolites. However, structural considerations derived from quantum mechanical calculations suggest that PhIP metabolites should groove-bind as well.

EXPERIMENTAL PROCEDURES

Chemicals

Caution: The heterocyclic aromatic amine PhIP is carcinogenic in rodents and should be handled carefully according to appropriate Environmental Safety and Health protocols. PhIP was purchased from Toronto Research Chemicals (Downsview, Ontario, Canada) and used without further purification, and DNaseI and S_1 nuclease were obtained from Boehringer Mannheim Biochemicals (Indianapolis, IN).

Preparation of DNA for spectroscopies

High molecular weight calf thymus DNA was purchased from Sigma Chemical, Inc. (St Louis, MO), and re-purified by incubation with Proteinase K (Sigma) followed by phenol extraction. Traces of phenol were eliminated from the DNA by three 70% ethanol washes, followed by dialysis against 4 l cold TE buffer [10 mM Tris−HCl (pH 7.8) with 1 mM Na_2EDTA] for 48 h using Spectra-Por membrane from Spectrum (Houston, TX) with a molecular weight cut-off of 1000 Da. DNA showed no phenol contamination as measured by UV spectroscopy.

DNA used for UV spectrophotometry was assayed to be ~12 000 base pairs (bp) median size after purification by phenol extraction and dialysis. DNA used in the fluorescence quenching, ^{31}P NMR and some ^{1}H NMR protocols was prepared by sonicating for 4−5 h, or until the median length of the DNA polymer was reduced to ~1000 bp.

To achieve the much smaller polymer sizes (~35 bp) needed for ^{1}H NMR spectroscopy of DNA imino protons, we modified the protocol of Kearns and co-workers (35,36). Highly polymerized DNA was resuspended in 1× DNaseI buffer [15 mg/ml DNA in 20 mM Tris−HCl (pH 7.4) and 10 mM $MnCl_2$]. DNaseI was added to 0.15 units DNaseI/ml, and the reaction proceeded for 17.5 min at 37°C. The reaction was stopped by the addition of Na_2EDTA to 25 mM, and the enzyme was removed by phenol extraction. Following precipitation by 2 vol cold (−20°C) ethanol, the DNA was resuspended in S_1 nuclease buffer [50 mM sodium acetate (pH 4.6), 280 mM NaCl, and 4.5 mM $ZnCl_2$]. To insure that the DNA was blunt-ended, DNA (6 mg/ml) and S_1 nuclease (4.6 units/ml) were incubated together at 37°C for 2.5 h. Enzyme was inactivated by addition of Na_2EDTA to 25 mM final concentration, and removed by phenol extraction. The DNA was dialyzed extensively against ice-cold NMR buffer [dibasic sodium phosphate (pH 7.0) and 100 mM NaCl]; then DNA sizes were assayed by agarose gel electrophoresis and were estimated to vary from 15−150 bp, with a median fragment size of ~30−35 bp. The DNA stained well with ethidium, and exhibited a hyperchromism at 260 nm of 38−40 %, indicating that little of the DNA was single-stranded (data not shown).

^{1}H NMR spectroscopy

Proton NMR spectra of PhIP−DNA complexes were generated at 300.13 MHz on a Bruker 300 MSL spectrometer, using 1331 or 11 pulse sequences for solvent signal suppression when required for H_2O solutions. Spectra were generated under the following conditions: 1000−40 000 scans depending on concentration of analyte; 1 s pulse repetition time; 9400 Hz spectral width; 16 K transform zero-filled to 32 000 data points; and 0.2−0.5 Hz (PhIP protons) or 4−20 Hz (DNA imino protons) line broadening preceding the Fourier transform, depending on the signal-to-noise (S/N) of the spectrum. The chemical shifts of the proton resonances were compared to the water proton resonance, which was assigned a value of $\delta = 4.8$ p.p.m. at 25°C. Both imino and water proton resonances exhibited temperature-dependent chemical shifts, which were referenced to TSP (3-trimethylsilyl-tetradeutero-sodium propionate) as a standard. The standard deviations of the proton chemical shifts were 0.01−0.05 p.p.m., depending on S/N.

PhIP aromatic protons in the presence of DNA were monitored at varying DNA concentrations by dissolving PhIP and ~1000 bp DNA in D_2O buffer [20 mM dibasic phosphate (pH 7.0) and 100 mM NaCl in 99.996 % isotopically pure D_2O from Sigma Chemical]. First the appropriate quantity of PhIP stock was pipetted into Eppendorf tubes. Then varying concentrations of DNA in 0.7 ml ^{1}H NMR buffer [20 mM dibasic phosphate (pH 7.0), and 100 mM NaCl] were added to the PhIP in Eppendorf tubes, followed by evaporation to dryness in a SpeedVac Concentrator (Savant Instruments, Inc., Farmingdale, NY). Finally 0.7 ml of D_2O was added to each sample. For all samples, the PhIP concentration was 200 mM, with DNA concentrations of 0.0, 1.0, 2.0 or 4.0 mM. The samples were maintained at 35°C during the acquisition of NMR data.

PhIP−DNA samples for the downfield DNA imino proton spectra were similarly prepared, except that the solvent was 90% H_2O and 10% D_2O. DNA concentrations of the five samples were 25, 12.5, 6.25, 2.5 and 1.25 mM, while PhIP concentrations were 83, 167, 208, 200 and 200 μM, respectively, corresponding to PhIP/DNA base pair ratios of 1/150, 1/75, 1/30, 1/12.5 and 1/6.25. Spectra of this last PhIP−DNA solution (1 PhIP/6.25 bp) were acquired with NMR probe temperatures varying from 283 K to 333 K (data not shown). Spectra of the other solutions were acquired at 308 K only. Fewer spectrum acquisitions (< 1000 scans) were possible if the DNA concentration was > 10 mM, but at 35°C, the maximum PhIP solubility was ~250 μM, yielding a PhIP/bp ratio of only 0.025 for 10 mM base pairs. Samples of higher PhIP/bp ratios required the same concentration of PhIP, but less DNA. Thus NMR spectra of such samples required large numbers of acquisitions.

^{31}P NMR spectroscopy

Phosphorus NMR spectra of PhIP−DNA solutions were obtained at 121.496 MHz on an MSL 300 instrument from Bruker Instruments, Inc. (Billerica, MA) according to the following parameters: typically 30 000 scans; $\pi/2$ pulse of 12 μs and 13 s between pulses; waltz broad-band proton decoupling; 2K transform zero-filled to 16K, 5000 Hz spectral width; and 10 Hz line broadening applied before Fourier transform. Long

acquisition times were required because PhIP is relatively insoluble in aqueous solutions; hence the DNA concentration was also kept low to maintain a high PhIP/bp DNA ratio. The standard deviations of the chemical shifts were ≤ 0.05 p.p.m. depending on S/N.

Sonicated calf thymus DNA with or without PhIP was dissolved in 20 mM Tris−HCl buffer (pH 7.8) with 100 mM NaCl and 1.0 mM Na_2EDTA. DNA was 4.5 mM in phosphates, and PhIP, if added, was either 125 or 270 μM. PhIP−DNA solutions were maintained at 25°C during mixing, and were pipetted into 10 mm NMR tubes and maintained in a probe at 35°C. DNA phosphate chemical shifts were measured with respect to trimethyl phosphate as an internal chemical shift standard.

Absorbance spectroscopy

Double-stranded calf thymus DNA of high molecular weight was added to PhIP solutions in buffer [20 mM Tris−HCl (pH 7.8), 100 mM NaCl, and 1 mM Na_2EDTA]. The final PhIP concentration was 25 μM, and the final DNA concentrations in base pairs ranged from 0.0−900 μM, corresponding to DNA bp/PhIP ratios of 0.0−36. Samples were kept in the dark at 35°C for 45 min to insure that binding reached equilibrium. PhIP−DNA complexes were maintained at 35°C by a water-jacketed cuvette holder. Samples were placed in 4 ml quartz cuvettes (1 cm optical pathlength) and scanned from 200−450 nm using a Shimadzu UV-2101PC UV/vis spectrophotometer. To obtain good resolution of the absorbance spectra, the scan speed was set at 100 nm/min, the sampling interval was 0.5 nm and the slits were set to 0.5 nm bandpass.

Fluorescence quenching

Fluorescence spectra were acquired with a Fluorolog-2 spectrofluorometer from Spex Industries, Inc. (Edison, NJ). All excitation and emission slits were 1.0 mm (3.87 nm bandpass) and emission spectra were generated as the average of three scans. The excitation wavelength was 315 nm (the absorbance maximum of PhIP) and the fluorescence emission was scanned from 330−450 nm, with data acquisition 0.2 s per nm increment. Samples monitored for luminescence were in 4 ml quartz cuvettes (1 cm optical pathlength) and were maintained at 25°C by a variable temperature cell holder from Spex Industries.

Quencher [either varying volumes of 5 mM silver nitrate ($AgNO_3$) or 6.86 M acrylamide] was titrated into magnetically stirred PhIP solutions with or without DNA. The PhIP concentration was 250 nM, and the DNA, where added, was 50 μM bp. Spectra were obtained 2−3 min after quencher was added each time. Quenching with silver ion was performed at low Ag^+/base ratios (0.025−0.3) in 10 mM sodium cacodylate (pH 7.0), and results in effective fluorescence quenching if ligand is inaccessible to solvent, e.g. an intercalated compound. Under the low salt, low Ag^+/base ratios used in this study, the silver ion is tightly complexed to DNA bases, especially guanines, with very little free silver in solution. Acrylamide, which efficiently quenches ligand exposed to solvent, was also titrated into PhIP solutions, yielding acrylamide concentrations of 20−500 mM. The resulting fluorescence intensities were corrected for the slight (< 7.5%) increase of sample volume upon addition of acrylamide. Samples for acrylamide quenching were in a buffer with ionic strength commensurate with the other buffers used in the NMR studies, i.e. 50 mM sodium cacodylate (pH 7.0), 100 mM NaCl, and 1 mM Na_2EDTA.

Computation of optimized PhIP structures

Semi-empirical quantum mechanical calculations. Optimized structures of PhIP, *N*-OH-PhIP, and *N*-acetoxy-PhIP were calculated by the Austin Model 1 (AM1) semi-empirical method (37) which uses experimental constraints in formulating the Hamiltonian. PhIP, *N*-OH-PhIP, and *N*-acetoxy-PhIP were constructed by the Spartan 2.0 software package from Wavefunction (Irvine, CA) using standard bond angles and distances, except that the torsional angle between the phenyl and imidazopyridine (IP) was varied for the initial structures. Calculations were performed by the Spartan software package on Iris Indigo workstation from Silicon Graphics (Mountain View, CA). The final structures obtained were the same regardless of the initial value of the torsional angle between the phenyl and the IP moieties.

Ab initio quantum mechanical calculations. The PhIP structure was constructed by the Spartan program using default parameters for bond angles and distances. This structure was fully optimized at the Hartree−Fock level of theory with a 6-31G* basis set using the Spartan quantum chemistry program. Starting with this optimized PhIP structure, in which the torsional angle between

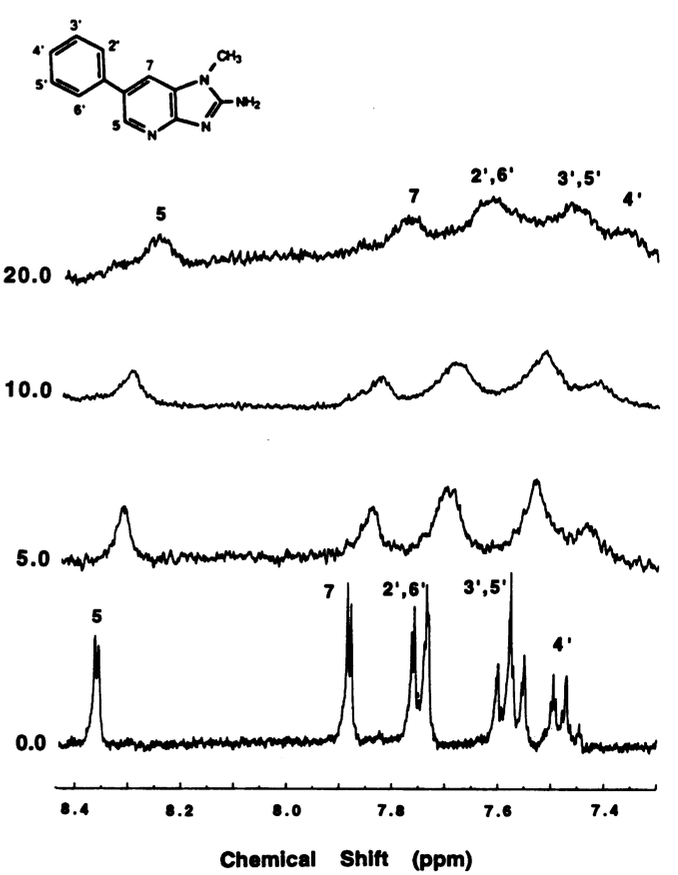

Figure 1. Aromatic region of the PhIP−DNA ^1H NMR spectrum, showing the resonances from PhIP protons. The lower spectrum is of PhIP in phosphate buffer, and the upper three spectra are of PhIP + varying concentrations of ~1000 bp DNA in phosphate buffer (D_2O solvent). The DNA bp/PhIP ratios are given to the left of each spectrum. All spectra were generated at 35°C.

the phenyl and IP moieties was 45 degrees, the phenyl-pyridine torsional potential energy surface was calculated. All other bond lengths, angles, and torsions were held fixed at their previously optimized values while the phenyl ring torsion was incremented at 5 degree intervals and the 6-31G* Hartree–Fock energy computed using the Gaussian 92 software package (Gaussian, Inc., Pittsburgh, PA). This yielded a 4.3 kcal/mole barrier to planarity. Such 'constrained' torsional energy surfaces are usually accurate, since for a small, rigid molecule, the other bond lengths, angles, and torsions do not significantly change as a single torsional angle is changed. To confirm this, in a second computation the PhIP structure was completely reoptimized with the phenyl and pyridine constrained to be co-planar. Because of a modest degree of molecular relaxation that occurred while the phenyl and pyridine rings were maintained co-planar, the energy of this re-optimized PhIP was 0.9 kcal/mole less than the starting co-planar structure. Thus a more accurate prediction of the barrier to co-planarity is 3.4 kcal/mole, verifying that there is a significant energy cost to forming the co-planar structure.

RESULTS

NMR studies of PhIP–DNA complexes

PhIP aromatic proton resonances broadened significantly and shifted slightly upfield upon addition of DNA (Figure 1) but could not be detected above background if the DNA bp/PhIP ratio was > 20. Thus, at 20 bp/PhIP it is likely that most or all of the PhIP was bound to the DNA, given the moderately high concentrations of PhIP and DNA needed for the NMR experiments. All PhIP aromatic protons, whether on the unconjugated phenyl moiety (protons 2′–6′) or on the pyridine (protons 5 and 7, Figure 1), shifted equivalently (0.11–0.12 p.p.m.) upfield upon the addition of DNA. This small upfield shift of the PhIP aromatic proton resonances demonstrates that PhIP binds to DNA, but the magnitude of the shift is ≥ four times smaller than expected for intercalative binding, and is consistent with a groove-binding mode of interaction (38–41).

The phosphorus resonance of calf thymus DNA (Figure 2) without PhIP was fairly broad (FWHM = 112 Hz). Upon addition of PhIP to the DNA, the resonance of the complex (1 PhIP/9 bp) was broadened by a factor of two with respect to unbound DNA (FWHM of 232 Hz versus 112 Hz). Because of the low PhIP solubility, it was difficult to achieve higher PhIP/bp molar ratios. Furthermore, there was a small 0.2 ± 0.05 p.p.m. upfield shift of the phosphorus resonance of PhIP–DNA complexes. A second peak was not generated upon addition of PhIP (upper spectrum), suggesting that PhIP is in fast exchange with the DNA. The chemical shift of DNA phosphates is a sensitive function of the DNA backbone torsional angles (42,43), and the data suggests a non-intercalative mode of DNA binding by PhIP since ligand-base stacking interactions consistently induce downfield shifts in the phosphorus resonances (42–45).

Lowfield ^{1}H NMR spectra of thymine and guanine imino protons of A–T and G–C base pairs, respectively, can be used to unambiguously elucidate, on a low-resolution level, the mode, kinetics, and specificity of DNA binding by small ligands (35,36). DNA *binding modes* can be determined by the chemical shift of the imino protons as intercalative, groove-binding, or 'non-specific outside' (35,36). The *kinetics*, or time of ligand residence on DNA, can be characterized as fast or slow, relative to the NMR experiment time scale, i.e., by observing the separation of peaks expressed in reciprocal frequency units. The *specificity*

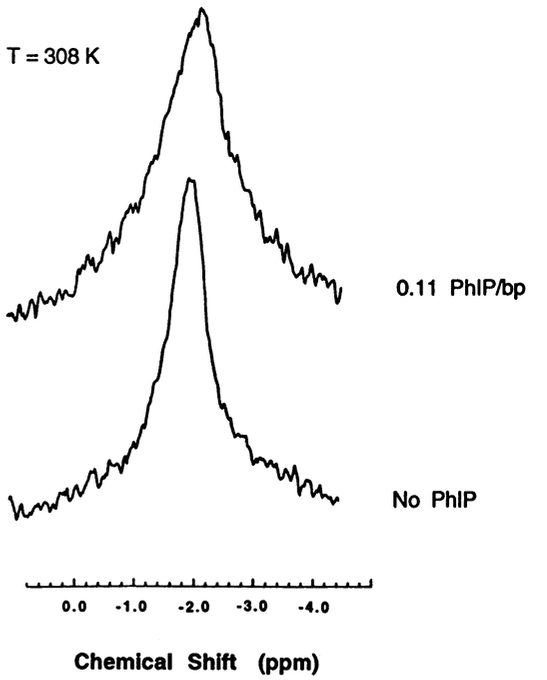

Figure 2. ^{31}P NMR spectroscopy of PhIP–DNA complexes. The temperature of the probe was maintained at 35°C, and trimethyl phosphate was added as an internal standard. Lower spectrum: 4.5 mM DNA (in phosphates). Upper spectrum: 4.5 mM DNA phosphates + 126 μM PhIP.

of binding may be interpreted as A–T or G–C specific, depending on whether the imino proton envelope corresponding to the A–T or G–C base pairs exhibits the greatest perturbation upon binding by PhIP. A highly detailed discussion of spectrum interpretation is given in refs 35 and 36.

In this study, we obtained excellent resolution between the G–C and A–T resonances at 35°C (Figure 3). The addition of PhIP shifted A–T and G–C resonances slightly downfield by 0.20 ± 0.05 and 0.15 ± 0.05 p.p.m., respectively. These data are commensurate with what is typically observed for groove-binders, which induce small downfield shifts of the imino resonances (36). By contrast, intercalators induce large (~1 p.p.m.) upfield shifts of the DNA imino proton resonances. Further, PhIP was determined to be slightly A–T specific, since the thymine imino proton resonance was shifted downfield to a greater degree than the guanine imino proton resonance. An A–T specificity of DNA binding has been reported for groove-binding molecules (46–48). The imino proton resonances were not appreciably broadened, and no additional peak appeared. Thus, PhIP appears to be in fast exchange with the DNA. We also acquired imino proton spectra of PhIP–DNA non-covalent complexes (data not shown) at temperatures ranging from 15–60°C. All spectra showed fast kinetics down to 15°C.

Absorbance spectra of PhIP–DNA complexes

The UV spectrum of PhIP in water (pH 7.0) at 37°C is shown on Figure 4A. Four prominent absorbance bands were detected at 314.5, 271.5, 225 and 208.5 nm, with corresponding molar extinction coefficients [ε(λ)] of 17 700, 8300, 27 400 and 26 000 M^{-1} cm^{-1}, respectively. The DNA absorbance severely overlapped most of the PhIP UV spectrum (Figure 4B), but the

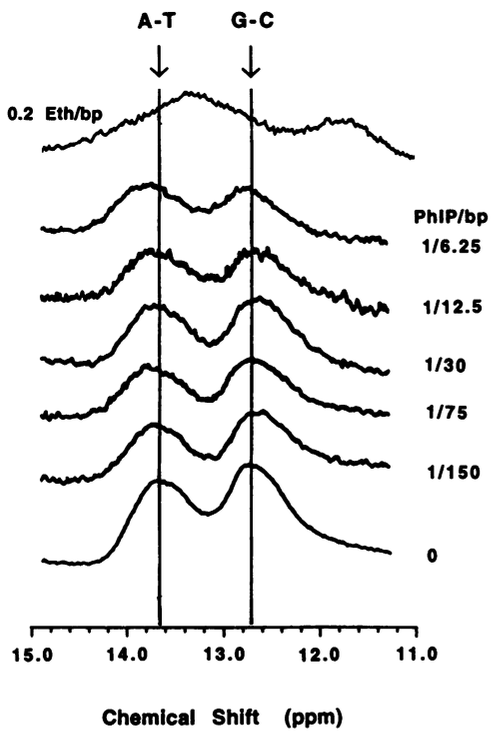

Figure 3. Downfield region of the ^1H NMR spectra of PhIP–DNA complexes showing resonances from DNA imino protons. To the right of each spectrum, the PhIP/DNA base pair ratio is given. The bottom spectrum is of DNA with no PhIP, whereas the top spectrum is of DNA + ethidium cation (0.2 Eth^+/bp). The ethidium–DNA complex was used as a standard since ethidium is a known intercalator under the solution conditions utilized in these experiments.

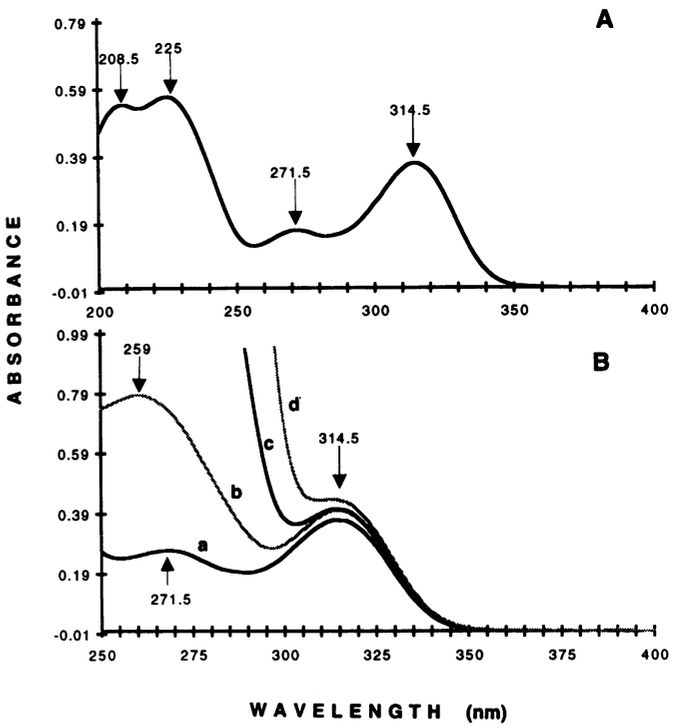

Figure 4. Panel **A**: UV spectrum of 25 μM PhIP in water, pH 7.0. Panel **B**: UV spectra monitoring the titrations of 25 μM PhIP with 2.5 μM DNA (spectrum a), 62.5 μM DNA (spectrum b), 250 μM DNA (spectrum c) and 900 μM DNA (spectrum d) in Tris buffer (pH 7.8).

lowest energy band of PhIP (λ_{max} = 315 nm) did not overlap the lowest energy $\pi \rightarrow \pi^*$ absorbance band of DNA (λ_{max} = 260 nm).

S_1 states of aromatic molecules are usually sensitive to electronic environment, with the lowest-energy absorption band undergoing considerable hypochromicity and red-shifting if the molecule's π electrons interact with the DNA base π electrons by intercalation (49–51). The 315 nm PhIP absorption band, within the resolution of the experiment, neither shifted to lower energy nor decreased in intensity (Figure 4B) upon addition of DNA. This result was also valid if the solution concentrations of analyte were equal those used for NMR experiments (see Figures 1–3), where binding was observed. Thus, since PhIP forms physical complexes with DNA, these data suggest that PhIP binds to the exterior of the DNA helix. However, the PhIP band at λ = 315 nm was very broad [full width at half-maximum (FWHM) = 3700 cm^{-1}], and small perturbations of the spectrum induced by DNA binding might be undetectable.

Fluorescence quenching of PhIP–DNA complexes

Silver ion (52–54) is a fluorescence quencher of solvent-inaccessible (intercalator) ligand species. Acrylamide (55) quenches the fluorescence from some groove-bound DNA adducts, although not necessarily the fluorescence from groove-bound fluorophores non-covalently complexed to DNA. Both acrylamide in the millimolar domain and silver ion in the micromolar domain strongly quenched PhIP fluorescence if DNA was not present (Figure 5). The fluorescence from PhIP in the presence of DNA was unquenched by Ag^+ ion (Figure 5A) at low r ratios ($r \leq 0.075$ mole Ag^+/mole DNA base), but was moderately quenched at higher ratios ($r = 0.1-0.3$ Ag^+PhIP/base). Even at the higher r ratios, PhIP exhibited much greater fluorescence than if DNA were absent. These data suggest that DNA protected the PhIP molecule from quenching by silver ion, and that PhIP was bound to DNA in a solvent-accessible orientation. On the other hand, acrylamide slightly increased the quenching of PhIP fluorescence if DNA was present in solution (Figure 5B). Acrylamide quenches the fluorescence from solvent-accessible (groove-bound) adduct better than it quenches the fluorescence from groove-bound or intercalated non-covalent ligands (55). Yet, since PhIP binding to DNA is weak, we believe these data are not inconsistent with a groove-binding or helix-external mode of PhIP binding to DNA.

DISCUSSION

In these studies, we used low-resolution NMR, absorbance and fluorescence spectroscopic techniques to evaluate the non-covalent DNA binding by the heterocyclic amine carcinogen PhIP. All methodologies implicated PhIP as a groove-binding molecule under the experimental conditions applied in this study. Further, PhIP binding was slightly A–T specific, and the molecule was in fast exchange with the DNA at temperatures above 15°C.

When PhIP was added, DNA imino proton and phosphorus resonances exhibited the respective downfield and upfield shifts characteristic of groove-binding. The absorbance and

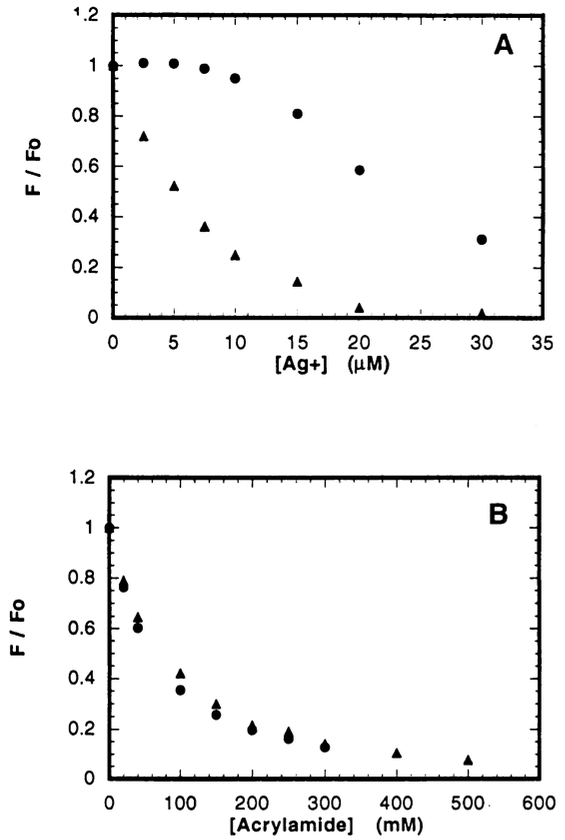

Figure 5. Quenching of PhIP luminescence by silver ion (Panel **A**) and acrylamide (Panel **B**). The top curve in Panel A (●) depicts the fluorescence quenching of 250 nM PhIP + 50 μM DNA bp (100 μM bases), and the bottom curve (▲) shows PhIP fluorescence quenching in the absence of DNA. Panel **B** shows acrylamide quenching with (●) and without (▲) 50 μM DNA. T = 298 K, all slits = 3.87 nm bandpass, and the excitation was at 315 nm with the intensity measured at the maximum of the fluorescence emission (usually 369 nm). The major Raman band of water was at 353 nm and did not affect the intensity measurement.

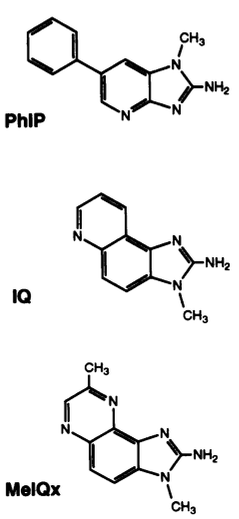

Figure 6. Structures of the heterocyclic amine food mutagens PhIP, IQ and 8-MeIQx.

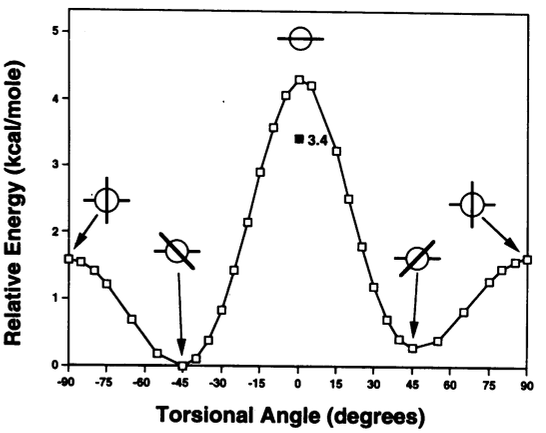

Figure 7. The torsional energy surface of PhIP calculated as Self-Consistent Field (SCF) 6-31G* energies, holding all bond angles, distances, and torsions fixed except for the phenyl-IP torsional angle. Note that the higher-level *ab initio* quantum calculation yields a preferred angle of 45 degrees, compared to 40 degrees for the semi-empirical AM1 calculation. The solid square at x,y = 0 degrees and 3.4 kcal/mole shows the energy barrier to phenyl rotation after re-optimization of the PhIP molecule holding the phenyl and IP moieties co-planar. The rest of the molecule relaxes slightly (0.9 kcal/mole) and the barrier is lowered to 3.4 kcal/mole.

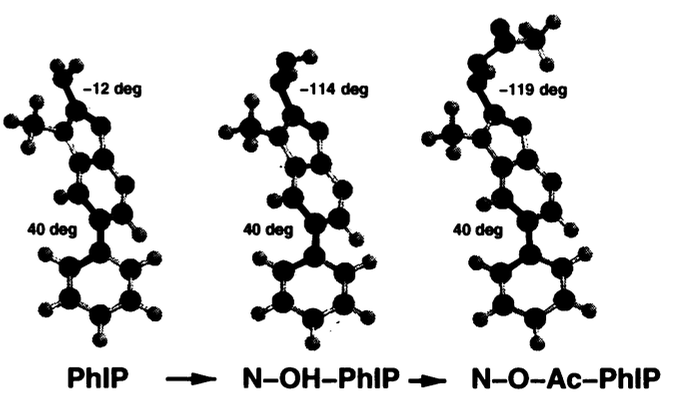

Figure 8. The structures of PhIP and its metabolites as calculated by semi-empirical quantum mechanical (AM1) calculations. Dihedral angles demonstrating the twist of the imidazopyridine skeleton with respect to the phenyl ring (bottom angle) or reactive group (top angle) are highlighted. The arrows at the bottom indicate the direction of metabolic activation *in vivo*.

fluorescence excitation bands of PhIP were unchanged when DNA was added and λ_{max} of the PhIP fluorescence emission from PhIP−DNA complexes (data not shown) was independent of the excitation wavelength within experimental resolution. That is, there were no apparent PhIP species possessing absorbance bands of significantly different energy than unbound PhIP. However, we cannot exclude that a base-stacked non-covalent binding mode might exist with a quantum yield near zero, as is the case of BPDE (50). If so, this would be a minor binding mode since the NMR and absorbance data do not indicate intercalation. Here we note that benzo[*a*]pyrone tetraols (BPTs) may have a minor external type of non-covalent DNA binding which induces no change in absorbance or fluorescence spectra (56). Finally, DNA-bound PhIP is very efficiently quenched by

acrylamide, an external quencher, but, compared to free PhIP, is much less effectively quenched by silver ion, an internal quencher.

The ^{1}H NMR of PhIP's aromatic protons also indicates a groove-bound molecule at physiological temperatures. However, since partial intercalation may produce modest upfield shifts in aromatic proton resonances (57), we cannot completely exclude that partial intercalation of PhIP may be occurring. In general, upon physical complexation with DNA, the aromatic protons of intercalators shift significantly upfield (0.5−1.0 p.p.m.), while those of groove-binding ligands shift slightly upfield or downfield (38−41,46,58). For a molecule with hybrid DNA binding characteristics, upfield and downfield chemical shifts may be observed for the same molecule. Ethidium provides an example: the aromatic protons of the base-stacking phenanthridinium ring shift upfield > 0.5 p.p.m., while the protons of the minor-groove-binding phenyl shift upfield < 0.2 p.p.m. (38,39). All PhIP aromatic protons, whether phenyl or on the pyridine, exhibited the same small chemical shift upon DNA binding, suggesting that most of the PhIP molecule is influenced equally by the solution environment. Thus, it is unlikely that the PhIP phenyl group protrudes into one of the grooves while the rest of the molecule intercalates.

Some quinoline and quinoxaline heterocyclic amines (e.g. IQ and MeIQx) appear to bind DNA by intercalation (59). Antibiotics of the triostin and quinomycin classes function as bisintercalators, where two quinoline or quinoxaline moieties base-stack into DNA (60,61). Since these belong to the same AIA class of heterocyclic amines as PhIP, one might ask why PhIP binds in a groove of DNA. In the section that follows, we used computational methods based on molecular quantum mechanics to address this issue. These calculations alone are insufficient to establish mode of DNA binding, but they can address issues raised by the experimental results.

Most heterocyclic amines, including MeIQx and IQ, are fully planar aromatic structures (Figure 6), with no bulky out-of-plane functionality that might impede intercalation between DNA bases. PhIP however possesses a phenyl moiety which is not necessarily co-planar with the main bicyclic imidazopyridine (IP) moiety of the molecule (Figures 1 and 6). PhIP has many resonance structures, but for most the phenyl ring at the 6-position is not conjugated with the IP skeleton of the PhIP molecule; hence, there is no reason to assume co-planarity of the phenyl moiety with the IP portion of the PhIP molecule. Indeed, *ab initio* and AM1 semi-empirical calculations show that PhIP and its metabolites possess phenyl rings with dihedral angles of 45° and 40°, respectively, between the phenyl and the IP skeleton of the PhIP molecule (Figures 7 and 8). In principle, steric effects produced by unfused phenyl groups may not interfere with intercalation (40,62). However, the large 40−45° dihedral angle between the two ring planes in PhIP and its metabolites (Figures 7 and 8), and the small size of the IP moiety (63), may preclude the carcinogen from forming good base-stacking contacts rendering the intercalation mode less favorable by PhIP.

A question arises as to whether the phenyl ring may be easily rotated to co-planarity with the IP moiety, since the phenyl is unconjugated. If so, PhIP and its metabolites would be more likely candidates as DNA intercalators. However, for a co-planar PhIP structure, the distance between the phenyl hydrogens (2′ and 6′, see Figure 1) and the IP hydrogens (5 and 7, see Figure 1) were computed by *ab initio* quantum theory to be less than the sum of the van der Waals radii of the atoms. Thus the debit of energy needed to rotate the phenyl to 0° is 3.4 kcal/mole, rendering such a possibility unlikely (Figure 7). But the relative torsional energy required to rotate the phenyl perpendicular to the IP ring was only 1.6 kcal/mole. Thus, we do not believe that the phenyl ring rotates to co-planarity upon DNA binding, suggesting that PhIP and its carcinogenic metabolites will not intercalate into DNA. Indeed, conformational modeling of the dG-C8-PhIP adduct using potential energy minimization searches (64) has led to a lowest energy conformation in which the PhIP adduct is located in the B-DNA minor groove, with phenyl ring twisted 21° with respect to the IP structure.

We also showed that PhIP exerts a slight preference for binding to A−T base pairs. This is often reported for groove-binding molecules (46−48), but leads to the question of why the formation of *covalent* adducts by PhIP is principally at guanines, even though the *non-covalent* binding is not specific for GC-rich DNA. In principle, steric constraints may preclude covalent attachment to non-guanine bases, even though these have strong nucleophilic centers. Indeed, racemic (±)-*anti*-benzo[*a*]pyrene diol epoxide (BPDE) predominantely forms adducts at guanines, even though the binding affinity of BPDE to poly(dA-dT)·(dA-dT) is greater than to poly(dG-dC)·(dG-dC) (32). However, it is also possible that the PhIP metabolites have a different DNA-binding base specificity than parent PhIP.

In summary, DNA recognition by intercalation is thought to be the initial event in the adduction of DNA by activated aromatic carcinogens (32−34,59). However, PhIP, while highly carcinogenic in rats and mice, appears to bind by a groove-binding mode at physiological temperature. The type of binding may not prove as important as the simple fact of the interaction itself, provided that ligand electrophiles are in close proximity with reactive base nucleophiles. We wish to point out, however, that these were *in vitro* interactions studied at pH 7.0 or 7.8 and at ambient temperatures, and they occurred in the presence of moderate concentrations of monovalent cation. Thus, our results apply only to DNA binding under these conditions.

In the future, it would be helpful to quantify the PhIP binding affinity to random sequence DNA and to defined-sequence polynucleotides. Further, one could design NMR experiments using defined-sequence oligodeoxynucleotides which would yield higher-resolution structural and kinetic data. However, binding studies with random-sequence DNA, such as were undertaken in this work, represent a 'benchmark', where all potential DNA binding sites are represented.

For these studies, we used the parent PhIP molecule and not its metabolites, which are moderately to very unstable. The substitution of other functional groups at the amine may severely affect the affinity and base specificity of PhIP binding to DNA, especially if the electrostatic potential of the molecule is substantially altered. But bulkier acetylated (Figure 8) or sulfated ultimate carcinogens should, by steric considerations, prove less able to intercalate than the unsubstituted PhIP carcinogen.

ACKNOWLEDGEMENTS

We thank Dr Nick Winter and Ms Erin Whitney for performing the AM1 calculations and the Hartree−Fock optimization of the PhIP structure, and Dr Lars Dragsted of the Danish Toxicology Center for the kind gift of the PhIP. This work was performed under the auspices of the US Department of Energy by the Lawrence Livermore National Laboratory under contract no. W-7405-ENG-48 and partially supported by NIH grant CA55861.

REFERENCES

1. Skog,K., Knize,M.G., Felton,J.S., and Jagerstad,M. (1992) Mutat. Res., **268**, 191–197.
2. Jagerstad,M., Skog,K., Grivas,S., and Olsson,K. (1991) Mutat. Res., **259**, 219–233.
3. Felton,J.S., Knize,M.G., Shen,N.H., Andresen,B.D., Bjeldanes,L.F., and Hatch,F.T. (1986) Environ. Health Perspect., **67**, 17–24
4. Felton,J.S., and Knize,M.G. (1991) Mutat. Res., **259**, 205–217.
5. Zhang,X.-M., Wakabayashi,K., Liu,Z.-C., Sugimura,T., and Nagao,M. (1988) Mutat. Res., **201**, 181–188.
6. Knize,M.G., Cunningham,P.L., Griffin,E.A.,Jr., Jones,A.L., and Felton,J.S. (1994) Food Chem. Toxicol., **32**, 15–21.
7. Manabe,S., Suzuki,H., Wada,O., and Ueki,A. (1993) Carcinogenesis, **14**, 899–901.
8. Manabe,S., Tohyama,K., Wada,O., and Aramaki,T. (1991) Carcinogenesis, **12**, 1945–1947.
9. Peluso,P., Castegnaro,M., Malaveille,C., Friesen,M., Garren,L., Hautefeuille,A., Vineis,P., Kadlubar,F., and Bartsch,H. (1991) Carcinogenesis, **12**, 713–717.
10. Fuscoe,J.C., Wu,R., Shen,N.H., Healy,S.K., and Felton,J.S. (1988) Mutat. Res., **201**, 241–251.
11. Jagerstad,M., and Grivas,S. (1985) Mutat. Res., **144**, 131–136.
12. Nagao,M., Wakabayashi,K., Kasai,H., Nishimura,S., and Sugimura,T. (1981) Carcinogenesis, **2**, 1147–1149.
13. Becher,G., Knize,M.G., Nes,I.F., and Felton,J.S. (1988) Carcinogenesis, **9**, 247–253.
14. Knize,M.G., and Felton,J.S. (1986) Heterocycles, **24**, 1815–1819.
15. Thompson,L.H., Tucker,J.D., Stewart,S.A., Christensen,M.L., Salazar,E.P., Carrano,A.V., and Felton,J.S. (1987) Mutagenesis, **2**, 483–487.
16. Aeschbacher,H.U., Turesky,R.J. (1991) Mutat. Res., **259**, 235–250.
17. Ito,N., Hasegawa,R., Sano,M., Tamano,S., Esumi,H., Takayama,S., and Sugimura,T. (1991) Carcinogenesis, **12**, 1503–1506.
18. Ochiai,M., Kumiko,O., Wakabayashi,K., Sugimura,T., and Nagao,M. (1991) Jpn. J. Cancer Res., **82**, 363–366.
19. Wakabayashi,K., Nagao,M., Esumi,H., and Sugimura,T. (1992) Cancer Res., **52**, 2092s–2098s.
20. Esumi,H., Ohgaki,H., Kohzen,E., Takayama,S., and Sugimura,T. (1989) Jpn. J. Cancer Res., **80**, 1176–1178.
21. Turteltaub,K.W., Knize,M.G., Buonarati,M.H., McManus,M.E., Veronese,M.E., Mazrimas,J.A., and Felton,J.S. (1990) Carcinogenesis, **11**, 941–946.
22. Holme,J.A., Wallin,H., Brunborg,G., Soderlund,E.J., Hongslo,J.K., and Alexander,J. (1989) Carcinogenesis, **10**, 1389–1396.
23. Frandsen,H., Rasmussen,E.S., Nielsen,P.A., Farmer,P., Dragsted,L., and Larsen,J.C. (1991) Mutagenesis, **6**, 93–98.
24. Buonarati,M.H., Turteltaub,K.W., Shen,N.H., and Felton,J.S. (1990) Mutat. Res., **245**, 185–190.
25. Turesky,R.J., Lang,N.P., Butler,M.A., Teitel,C.H., and Kadlubar,F.F. (1991) Carcinogenesis, **12**, 1839–1845.
26. Alexander,J., Wallin,H., Rossland,O.J., Solberg,K.E., Holme,J.A., Becher,G., Andersson,R., and Grivas,S. (1991) Carcinogenesis, **12**, 2239–2245.
27. Takayama,K., Yamashita,K., Wakabayashi,K., Sugimura,T., and Nagao,M. (1989) Jpn. J. Cancer Res., **80**, 1145–1148.
28. Snyderwine,E.G., Schut,H.A.J., Adamson,R.H., Thorgeirsson,U.P., and Thorgeirsson,S.S. (1992) Cancer Res. (Suppl.), **52**, 2099s–2102s.
29. Lin,D., Kaderlik,K.R., Turesky,R.J., Miller,D.W., Lay,J.O.Jr., and Kadlubar,F.F. (1992) Chem. Res. Toxicol., **5**, 691–697.
30. Frandsen,H., Grivas,S., Andersson,R., Dragsted,L., and Larsen,J.C. (1992) Carcinogenesis, **13**, 629–635.
31. Turesky,R.J., Rossi,S.C., Welti,D.H., Lay,J.O.,Jr., and Kadlubar,F.F. (1992) Chem. Res. Toxicol., **5**, 479–490.
32. Geacintov,N.E., Shahbaz,M., Ibanez,V., Moussaoui,K., and Harvey,R.G. (1988) Biochemistry, **27**, 8380–8387.
33. Stone,M.P., Gopalakrishnan,S., Harris,T.M., and Graves,D.E. (1988) J. Biomol. Struct. Dyn., **5**, 1025–1041.
34. Meehan,T., Gamper,H., and Becker,J.F. (1982) J. Biol. Chem., **257**, 10479–10485.
35. Feigon,J., Leupin,W., Denny,W.A., and Kearns,D.R. (1982) Nucleic Acids Res., **10**, 749–762.
36. Feigon,J., Leupin,W., Denny,W.A., and Kearns,D.R. (1984) J. Med. Chem., **27**, 450–465.
37. Dewar,M.J.S., Zoebisch,E.G., Healy,E.F., and Stewart,J.J.P (1985) J. Am. Chem. Soc., **107**, 3902–3909.
38. Patel,D.J., and Canuel,L.L. (1976) Proc. Natl Acad. Sci. USA, **73**, 3343–3347.
39. Reinhardt,C.G. and Krugh,T.R. (1978) Biochemistry, **17**, 4845–4854.
40. Wilson,W.D., Tanious,F.A., Watson,R.A., Barton,H.J., Strekowska,A., Harden,D.B., and Strekowski,L. (1989) Biochemistry, **28**, 1984–1992.
41. Wilson,W.D., Tanious,F.A., Barton,H.J., Jones,R.L., Fox,K., Wydra,R.L., and Strekowski,L. (1990) Biochemistry, **29**, 8452–8461.
42. Gorenstein,D.G. (1981) Ann. Rev. Biophys. Bioeng., **10**, 355–386.
43. Wilson,W.D., Keel,R.A., and Mariam,Y.H. (1981) J. Am. Chem. Soc., **103**, 6267–6269.
44. Scott,E.V., Jones,R.L., Banville,D.L., Zon,G., Marzilli,L.G., and Wilson,W.D. (1988) Biochemistry, **27**, 915–923.
45. Reinhardt,C.G., and Krugh,T.R. (1977) Biochemistry, **16**, 2890–2895.
46. Lane,A.N., Jenkins,T.C., Brown,T., and Neidle,S. (1991) Biochemistry, **30**, 1372–1385.
47. Kopka,M.L., Yoon,C., Goodspell,D., Pjura,P., and Dickerson,R.E. (1985) Proc. Natl Acad. Sci. USA, **82**, 1376–1380.
48. Harshman,K.D. and Dervan,P.B. (1985) Nucleic Acids Res., **13**, 4825–4835.
49. Waring,M.J. (1965) J. Mol. Biol., **13**, 269–282.
50. MacLeod,M.C., Smith,B., and McClay,J. (1987) J. Biol. Chem., **262**, 1081–1087.
51. Bailey,S.A., Graves,D.E., Rill,R., and Marsch,G.A. (1993) Biochemistry, **32**, 5881–5887.
52. Prusik,T., Geacintov, N.E., Tobiasz, C., Ivanovic, V., and Weinstein, I.B. (1979) Photochem. Photobiol., **29**, 223–232.
53. Undeman,O. Lycksell, P.O., Gräslund,A., Astlind,T., Ehrenberg, A., and Jernström,B. (1983) Cancer Res., **43**, 1851–1860.
54. Kadlubar,F.F., Melchior, W.B.Jr., Flammang,T.J., Gagliano,A.G., Yoshida,H., and Geacintov,N.E. (1981) Cancer Res., **41**, 2168–2174.
55. Geacintov,N.E., Zinger,D., Ibanez,V., Santella,R., Grunberger,D. and Harvey,R.G. (1987) Carcinogenesis, **7**, 925–935.
56. Ibanez,V., Geacintov,N.E., Gagliano,A.G., Brandimarte,S. and Harvey,R.G. (1980). J.Am.Chem.Soc., **102**, 5661–5666.
57. Robledo-Luiggi,C., Wilson,W.D., Pares,E., Vera,M., Martinez,C.S., and Santiago,D. (1991) Biopolymers, **31**, 907–917.
58. Kumar,S., Yadagiri,B., Zimmermann,J., Pon,R.T., and Lown,J.W. (1990) J. Biomol. Struct. Dyn., **8**, 331–357.
59. Watanabe,T., Yokoyama,S., Hayashi,K., Kasai,H., Nishimura,S., and Miyazawa,T. (1982) FEBS Lett., **150**, 434–438.
60. Wang,A.H.-J., Ughetto,G., Quigley,G.J., Hakoshima,T., van der Marel,G.A., van Boom,J.H., and Rich,A. (1984) Science, **225**, 1115–1121.
61. Waring,M.J. and Wakelin,L.P.G. (1974) Nature, **252**, 653–657.
62. Jain,S.C., Tsai,C.C., and Sobell,H.M. (1977) J. Mol. Biol., **114**, 317–331.
63. Wilson,W.D., Wang,Y.H., Kusuma,S., Chandrasekaran,S., and Boykin,D.W. (1986) Biophys. Chem., **24**, 101–109.
64. Carothers,A.M., Yuan,W., Hingerty,B.E., Broyde,S., Grunberger,D., and Snyderwine,E.G. (1994) Chem. Res. Toxicol., **7**, 209–218.